

VU Research Portal

The development, structure and repair of articular cartilage

Hunziker, E.B.

2008

document version

Publisher's PDF, also known as Version of record

[Link to publication in VU Research Portal](#)

citation for published version (APA)

Hunziker, E. B. (2008). *The development, structure and repair of articular cartilage*.

General rights

Copyright and moral rights for the publications made accessible in the public portal are retained by the authors and/or other copyright owners and it is a condition of accessing publications that users recognise and abide by the legal requirements associated with these rights.

- Users may download and print one copy of any publication from the public portal for the purpose of private study or research.
- You may not further distribute the material or use it for any profit-making activity or commercial gain
- You may freely distribute the URL identifying the publication in the public portal ?

Take down policy

If you believe that this document breaches copyright please contact us providing details, and we will remove access to the work immediately and investigate your claim.

E-mail address:

vuresearchportal.ub@vu.nl

Variation of cell and matrix morphologies in articular cartilage among locations in the adult human knee

Thomas M. Quinn Ph.D.^{†*}, Ernst B. Hunziker M.D.[‡] and Hans-Jörg Häuselmann M.D.[§]

[†] Cartilage Biomechanics Group, Ecole Polytechnique Fédérale de Lausanne, Switzerland

[‡] ITI Research Institute, University of Bern, Switzerland

[§] Laboratory for Experimental Cartilage Research, Klinik im Park, Zürich, Switzerland

Summary

Objective: Understanding of articular cartilage physiology, remodelling mechanisms, and evaluation of tissue engineering repair methods requires reference information regarding normal structural organization. Our goals were to examine the variation of cartilage cell and matrix morphology in different topographical areas of the adult human knee joint.

Methods: Osteochondral explants were acquired from seven distinct anatomical locations of the knee joints of deceased persons aged 20–40 years and prepared for analysis of cell, matrix and tissue morphology using confocal microscopy and unbiased stereological methods. Differences between locations were identified by statistical analysis.

Results: Medial femoral condyle cartilage had relatively high cell surface area per unit tissue volume in the superficial zone. In the transitional zone, meniscus-covered lateral tibia cartilage showed elevated chondrocyte densities compared to the rest of the knee while lateral femoral condyle cartilage exhibited particularly large chondrocytes. Statistical analyses indicated highly uniform morphology throughout the radial zone (lower 80% of cartilage thickness) in the knee, and strong similarities in cell and matrix morphologies among cartilage from the femoral condyles and also in the mediocentral tibial plateau. Throughout the adult human knee, the mean matrix volume per chondron was remarkably constant at approximately 224,000 μm^3 , corresponding to approximately 4.6×10^5 chondrons per cm^3 .

Conclusions: The uniformity of matrix volume per chondron throughout the adult human knee suggests that cell-scale biophysical and metabolic constraints may place limitations on cartilage thickness, mechanical properties, and remodelling mechanisms. Data may also aid the evaluation of cartilage tissue engineering treatments in a site-specific manner. Results indicate that joint locations which perform similar biomechanical functions have similar cell and matrix morphologies; findings may therefore also provide clues to understanding conditions under which focal lesions leading to osteoarthritis may occur.

© 2005 OsteoArthritis Research Society International. Published by Elsevier Ltd. All rights reserved.

Key words: Human, Knee, Articular cartilage, Morphology.

Introduction

Articular cartilage has a highly specialized composition and structure which is adapted to serve its functions as a lubricating and load-bearing surface in synovial joints. Furthermore, within a cartilage layer, the superficial, transitional (middle) and radial (deep) zones exhibit variations in matrix biochemical composition, cell morphology, and cell–matrix structural organization as a function of depth^{1–3} (Fig. 1). These distinct tissue zones exhibit different biomechanical properties⁴ and rates of cell metabolic activities⁵, suggesting differential adaptations to distinct biomechanical roles. Chondrocyte biological activities are influenced by the local cell microphysical environment⁶. Therefore, cartilage structural organization appears to play a central role in determining biomechanical function, chondrocyte-mediated matrix deposition, and remodelling due to changes in tissue loading patterns.

Quantitative data regarding the microstructure of articular cartilage is useful for the understanding of tissue function in health and disease. Cartilage thickness, which contributes fundamentally to tissue biomechanical function, varies considerably throughout the human knee joint^{7–11}, likely due to its anatomical role in compensating for joint incongruence¹² and due to local differences in articular mechanics¹³. Short-term thickness changes in response to joint loading are rapid¹⁴ and site-specific¹⁵. Longer-term tissue remodelling responses to altered loading conditions appear to involve dramatic thinning under decreased load¹⁶, but only limited thickening under increased load^{8,11}. Cartilage adaptive potential is likely limited by cell-scale biophysics: adult chondrocytes rely heavily upon solute transport through the avascular extracellular matrix for their biological activities. Chondrocyte metabolism is therefore closely linked to the local transport environment which is in part determined by matrix structural organization¹⁷. Osteoarthritis (OA) can originate from highly focal lesions in weight-bearing joints¹⁸, possibly due to local differences in cartilage mechanical properties^{7,8}, or tissue microstructure. Therefore, normal cartilage physiology and OA can potentially be better understood if more detailed and site-specific morphological data are available. In addition, tissue

*Address correspondence and reprint requests to: T. M. Quinn, Cartilage Biomechanics Group, AA B019, EPFL, CH-1015 Lausanne, Switzerland. Tel: 41-21-693-83-50; Fax: 41-21-693-86-60; E-mail: thomas.quinn@epfl.ch

Received 12 September 2003; revision accepted 12 April 2005.

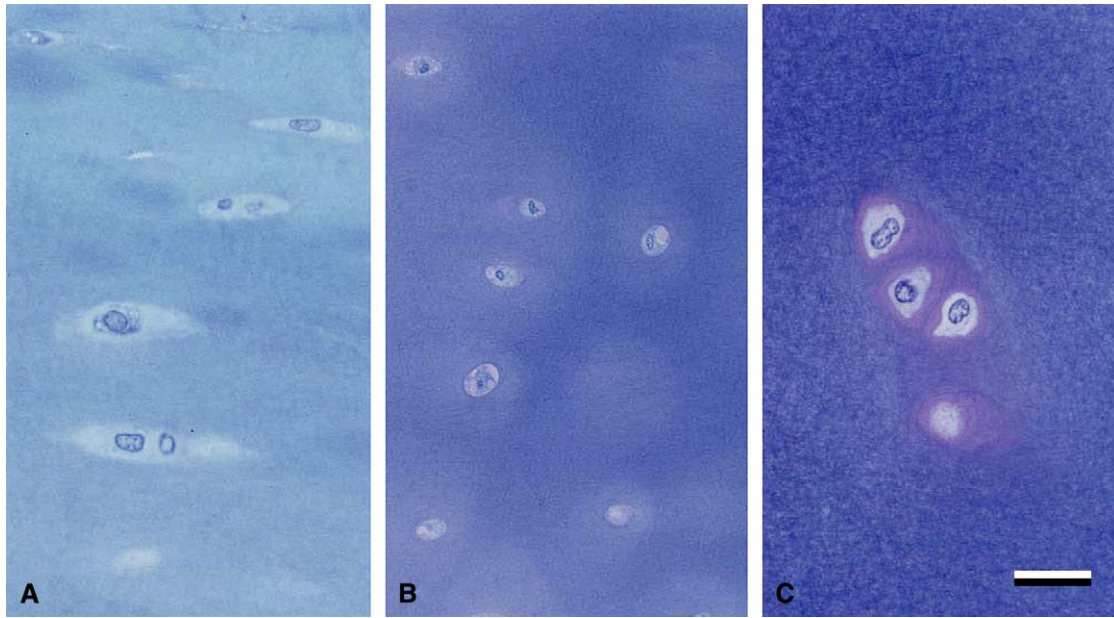


Fig. 1. Light micrographs of normal adult human articular cartilage originating from (a) the superficial zone, (b) the transitional zone, and (c) the lower radial zone. In the superficial zone, chondrocytes are relatively flattened and exhibit elliptical cross-sections. In the transitional zone, chondrocytes have a more rounded profile and in the lower radial zone they tend to be grouped in vertical stacks (chondrons) and show high variability in individual cell shapes. Semi-thin ($1\ \mu\text{m}$ thick) sections of Epon-embedded tissue stained with Toluidine Blue O. Bar = $20\ \mu\text{m}$.

engineering efforts may benefit from having detailed structural information for the original tissue (the “optimal solution”) as a reference point for evaluation. Noninvasive methods for individualized quantitative morphometry at the tissue scale show promise for clinical diagnostic applications in the future¹⁹, and could benefit from more detailed matrix morphometric data at sub-tissue length scales for comparison. With a view towards these varied applications, the aim of this study was to quantify and compare cell and matrix morphologies in articular cartilage obtained from seven well-defined locations in the human knee joint.

Methods

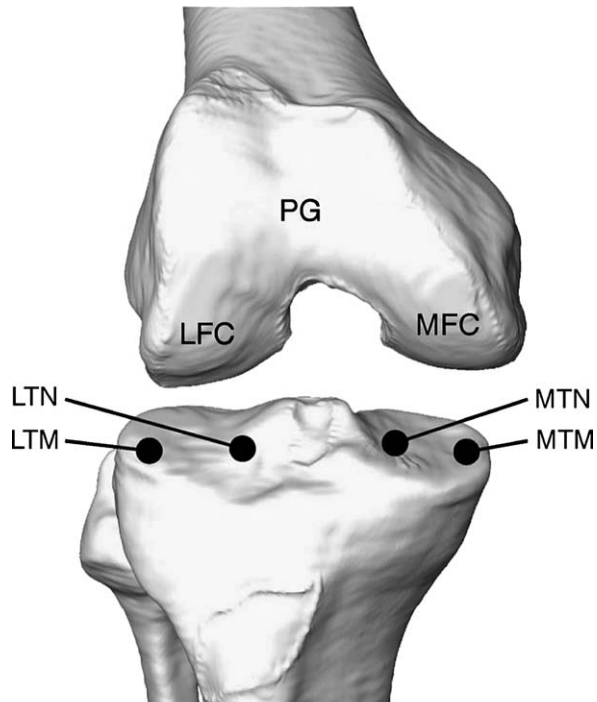
With the approval of the Medical Ethics Commission and the cooperation of the Department of Forensic Medicine of the University of Bern, articular cartilage samples were obtained from 10 adult humans (nine men aged 20–40 years and one woman aged 23 years). Subjects were victims of traffic accidents, suicide or drug overdose and had suffered from neither acute nor chronic disease. Tissue was removed within 48 h after death; all knee joints exhibited a healthy, glossy and intact articular surface. Two to three cylindrical osteochondral explants of 4 mm diameter were drilled perpendicular to the articular surface from seven distinct locations in the knee (Fig. 2): medial and lateral femoral condyles (MFC, LFC), patellar groove (PG), medial tibial plateau meniscus-covered and not meniscus-covered (MTM, MTN), and lateral tibial plateau meniscus-covered and not (LTM, LTN). Greater precision regarding definition of locations (superior to that suggested by Fig. 2) was limited by restrictions related to anatomical dissecting and the need to reconstitute the joint for ethical reasons. Nevertheless, locations were defined with similar precision to previous studies^{7,8,10,20}.

Immediately after biopsy, tissue cylinders were fixed in a solution of 5% glutaraldehyde (buffered with 0.1 M sodium

cacodylate, pH 7.4) over 1 week at ambient temperature. This fixation protocol results in autofluorescence which improves cell contrast during subsequent confocal microscopy. Explants were then stored in 70% ethanol at 4°C until microscopic examination (typically for a few days); this fixation and storage protocol has previously been shown to induce negligible deformation artifacts³.

On the day of examination, tissue cylinders were bisected vertically with a razor blade and the subchondral bone trimmed to $<1\ \text{mm}$ thickness, under continual immersion in 70% ethanol. Attachment to subchondral bone was preserved to minimize cartilage swelling. Vertical sections $100\ \mu\text{m}$ thick were then cut using a vibratome (EMS OTS 3000-03, Electron Microscopy Sciences, Fort Washington, PA, USA). Sections were kept bathed in 70% ethanol and sandwiched between a glass microscope slide and coverslip (sealed with nail polish) and used immediately for observation on the microscope.

A laser scanning confocal microscope (MRC 600 LSC imaging system; Bio-Rad, Hertfordshire, UK) was used at a zoom of one in conjunction with a $60\times$ oil-immersion objective (numerical aperture 1.4), an argon laser excitation source (488 nm) with a 510 nm longpass emission filter. Under light microscopy, the thickness of hyaline articular cartilage from the articular surface to the tidemark was measured and used to define three tissue zones: superficial (10% of thickness), transitional (10%), and radial (80% of tissue thickness). The radial zone was then further divided into four sub-zones (each 20% of tissue thickness). Within each tissue zone, stereological dissectors were obtained in the form of serial optical sections (confocal images covering an area of $180 \times 240\ \mu\text{m}^2$) spaced $5\ \mu\text{m}$ apart (at increasing depth of focus into the specimen). Four sequential scans were averaged to acquire a single image. These were photographed using colour slide film and projected to a final magnification of $870\times$ for stereological measurements. Two images were acquired per dissector in the



- MFC - Medial Femoral Condyle
- LFC - Lateral Femoral Condyle
- PG - Patellar Groove
- MTM - Medial Tibia (meniscus-covered)
- MTN - Medial Tibia (no meniscus)
- LTN - Lateral Tibia (no meniscus)
- LTM - Lateral Tibia (meniscus-covered)

Fig. 2. Anatomical sketch of human knee joint (distal femur and tibial plateau) illustrating the seven anatomical locations from which osteochondral explants were harvested.

superficial and transitional zones, and four images were acquired per dissector in each of the radial zones. Thicker dissectors were used for the radial zone ($15\ \mu\text{m}$ vs $5\ \mu\text{m}$ for the superficial and transitional zones) because this was more suitable for the stereological analysis of chondrons, which have a larger characteristic size than chondrocytes.

Established stereological methods^{21,22} were used for the estimation of four primary morphological parameters: chondrocyte volume per unit tissue volume (V_V), cell surface area per unit tissue volume (S_V), number of cells and number of chondrons per unit tissue volume (N_V and N_{Vc}). For V_V , a rectangular 10×10 grid of points covering a surface of $20.5 \times 15.6\ \text{cm}^2$ was placed over a single projected image, and the number of points “touching” cells was counted. This number (expressed as a percent) then immediately provided an estimator of V_V . For S_V , a rectangular 6×6 grid of cycloid arcs was placed over a projected image, and the number of intersections (I) with cell–matrix interfaces was counted. Then S_V was estimated as $2I/L^2$, where $L = 1.82\ \text{mm}$ was the total length of cycloid arcs in “image-space”. N_V and N_{Vc} were estimated as the number of cell or chondrons, respectively, which did not appear in the first image of a dissector, but which appeared in

subsequent images, divided by the dissector volume. The dissector surface used for determining N_V and N_{Vc} was delimited by a $134 \times 178\ \mu\text{m}^2$ bounding box. This was deliberately chosen to be smaller than the $180 \times 240\ \mu\text{m}^2$ images to allow for the consistent allocation of cells to rectangular blocks of tissue in 3D space: only cells or chondrons which appeared within the bounding box but did not touch its lower or left boundaries were included in the analysis.

Five secondary parameters were then estimated based on these primary ones including characteristic cell volume ($V = V_V/N_V$), cell surface area ($S = S_V/N_V$), matrix volume per cell ($M = 1/N_V - V$), number of cells per chondron ($N_c = N_V/N_{Vc}$), and matrix volume per chondron ($M_c = 1/N_{Vc} - N_c V$). For comparison to “Stockwell’s rule”²⁴, the total number of cells per unit articular surface (N_{AS}) was determined as the sum of $N_V d$ over all of the six tissue zones, where d represents the zone thickness. Similarly, the total number of chondrons per unit articular surface (N_{ASc}) was also determined.

Data were averaged over the 10 human specimens. Variations in morphological parameters between the seven distinct anatomical locations in the knee were examined by analysis of variance (ANOVA) with post hoc Tukey tests; results were considered significant for $P < 0.05$. Data are presented as mean \pm s.e.m. (n).

Results

Articular cartilage thickness measurements were consistent with previous findings^{7–11}. Thickness varied somewhat on the distal femur (between $2.4 \pm 0.2\ \text{mm}$ at the MFC and $2.9 \pm 0.2\ \text{mm}$ at the PG) and considerably more on the tibial plateau (between $2.2 \pm 0.1\ \text{mm}$ at the MTM and $4.0 \pm 0.2\ \text{mm}$ at the LTN) (Fig. 3). The MTM was significantly thinner than the PG, MTN, and LTN, while the LTN was significantly thicker than all other locations examined (Fig. 3).

In the superficial zone, cell densities appeared to be generally higher than in the deeper tissue zones, as expected³ (Table 1; statistical analysis of differences between zones not shown). Among the seven different locations in the knee examined, the most important differences in superficial zone morphology arose in association with the MFC. Cell surface area per unit volume (S_V) was significantly greater in the MFC vs the PG and vs both

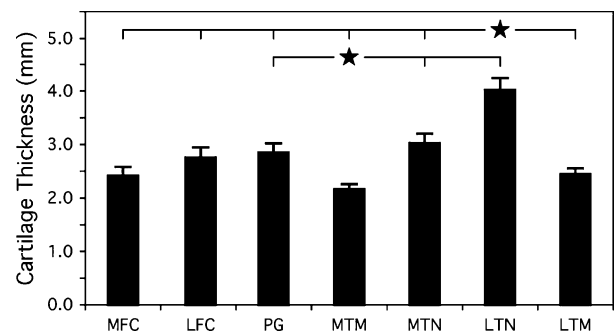


Fig. 3. Cartilage thickness at seven different anatomical sites in the human knee (mean \pm s.e.m., $n = 10$). Stars (★) indicate sites with significantly different thicknesses from those sites indicated by tick marks on the associated horizontal bars ($P < 0.05$).

Table I

Summary of results for cell and matrix morphological parameters measured within the superficial, transitional, and radial (deep) zones of cartilage from seven different locations in the adult human knee (mean \pm S.E.M.)

	V_v (%)	S_v (mm ⁻¹)	N_v (10 ³ mm ⁻³)	V (μ m ³)	S (μ m ²)	M (10 ³ μ m ³)	n
Superficial zone							
MFC	2.6 \pm 0.3	15.0 \pm 1.1**	24.0 \pm 3.2	1240 \pm 240	670 \pm 60	46 \pm 6	8
LFC	2.7 \pm 0.5	12.0 \pm 2.0	21.2 \pm 1.6	1220 \pm 150	550 \pm 60	48 \pm 4	6
PG	1.6 \pm 0.1	9.6 \pm 1.0*	18.4 \pm 1.4	890 \pm 100	520 \pm 40	57 \pm 4	10
MTM	2.0 \pm 0.4	8.9 \pm 1.4*	20.7 \pm 3.8	1150 \pm 280	460 \pm 40	60 \pm 8	10
MTN	1.7 \pm 0.3	9.1 \pm 1.1*	13.8 \pm 1.3	1200 \pm 200	650 \pm 60	76 \pm 8	8
LTN	2.1 \pm 0.3	10.0 \pm 1.1	16.7 \pm 2.5	1380 \pm 140	700 \pm 120	72 \pm 11	10
LTM	2.0 \pm 0.3	12.8 \pm 0.9	22.3 \pm 2.5	1040 \pm 200	620 \pm 70	48 \pm 5	8
Transitional zone							
MFC	2.1 \pm 0.2	9.0 \pm 0.6	10.3 \pm 4.7*	2090 \pm 220	880 \pm 60	97 \pm 5	8
LFC	2.1 \pm 0.4	8.9 \pm 1.0	9.0 \pm 1.3*	2640 \pm 560	1300 \pm 460**	137 \pm 41*	6
PG	2.2 \pm 0.3	8.3 \pm 0.7	13.7 \pm 0.6	1640 \pm 240	610 \pm 60*	72 \pm 3	10
MTM	1.2 \pm 0.2*	7.0 \pm 0.8*	9.6 \pm 0.9*	1280 \pm 180	760 \pm 80	113 \pm 13	10
MTN	1.3 \pm 0.3*	5.7 \pm 0.8*	9.0 \pm 1.0*	1590 \pm 410	690 \pm 130	119 \pm 12	8
LTN	1.6 \pm 0.2*	6.6 \pm 0.9*	10.2 \pm 0.9*	1630 \pm 230	670 \pm 70	108 \pm 16	10
LTM	2.7 \pm 0.3**	11.9 \pm 1.0**	17.8 \pm 1.9**	1600 \pm 160	680 \pm 30	60 \pm 8**	8
Radial zone							
MFC	1.5 \pm 0.3	6.8 \pm 0.9	7.7 \pm 0.8	2020 \pm 430	910 \pm 140	141 \pm 17	8
LFC	1.6 \pm 0.4	5.7 \pm 1.0	7.1 \pm 0.9	2600 \pm 1000	1110 \pm 680	184 \pm 76	6
PG	1.4 \pm 0.2	5.9 \pm 0.7	8.2 \pm 0.7	1790 \pm 340	750 \pm 90	133 \pm 14	10
MTM	1.1 \pm 0.2	5.1 \pm 0.7	6.9 \pm 0.6	1650 \pm 280	730 \pm 90	152 \pm 16	10
MTN	1.1 \pm 0.2	5.2 \pm 0.9	7.1 \pm 0.9	1530 \pm 290	730 \pm 90	148 \pm 17	8
LTN	1.1 \pm 0.2	4.9 \pm 0.7	6.8 \pm 0.7	1710 \pm 310	730 \pm 90	164 \pm 20	10
LTM	2.1 \pm 0.3	8.1 \pm 1.0	9.2 \pm 0.9	2410 \pm 370	900 \pm 90	117 \pm 12	9

MFC, medial femoral condyle; LFC, lateral femoral condyle; PG, patellar groove; MTM, medial tibial plateau (meniscus-covered); MTN, medial tibial plateau (not meniscus-covered); LTN, lateral tibial plateau (not meniscus-covered); LTM, lateral tibial plateau (meniscus-covered). V_v , chondrocyte volume per unit cartilage volume; S_v , chondrocyte surface area per unit cartilage volume; N_v , number of chondrocytes per unit cartilage volume; V , chondrocyte volume; S , chondrocyte surface area; M , matrix volume per chondrocyte. Statistical comparisons were calculated between locations (not between tissue zones). Within the data set for each morphological parameter and tissue zone, data marked by asterisks (*) are significantly different ($P < 0.05$) from the data marked by double asterisks (**).

locations in the medial tibia (MTM and MTN). These variations were consistent with the relatively high (but not significantly different in the statistical analysis) cell volume fraction (V_v), cell number density (N_v), and cell surface area (S) observed in the superficial zone of the MFC (Table I).

In the transitional zone, the most important differences in morphology arose in association with the LTM. The LTM exhibited significantly greater cell volume density (V_v), cell surface area density (S_v), and cell number density (N_v) compared to the rest of the tibial plateau (MTM, MTN, and LTN) and significantly greater cell number density also as compared to the femoral condyles (MFC and LFC). Consistent with these findings, matrix volume per cell (M) was smallest in the LTM, and significantly smaller than that measured for the LFC (Table I). This latter result appeared to be also related to the relatively high cell volumes (V) and surface areas (S) measured for the LFC wherein cell volume density did not exhibit "standout" behavior, so that matrix volumes per cell in the LFC were relatively high (Table I).

For the radial zones, statistical analyses performed for each of the nine morphological parameters within each of the seven anatomical locations indicated that data could be pooled and simplified. For each parameter and location, ANOVA was performed among the four radial zones; in only two cases (of the $9 \times 7 = 63$ ANOVAs performed) was significant variance indicated ($P = 0.0495$ at the LTN for V_v , and $P = 0.02$ at the MTM for N_v). Therefore, data which had been sampled from the four radial sub-zones were pooled into a single zone representing the deepest 80% of the cartilage layer.

Findings for the radial zone were dominated by a somewhat unique morphology of the LTM; however, no significant differences among locations in the knee were detected (Table I). Compared to all other locations examined, the LTM appeared to exhibit the highest cell volume density (V_v), cell surface area density (S_v), and cell number density (N_v). Remarkably, the "nearest neighbour" of the LTM, the LTN, consistently exhibited among the smallest values for V_v , S_v , and N_v . Similar to findings for the transitional zone, matrix volume per cell (M) in the radial zone appeared to be smallest in the LTM, while the LFC and MFC exhibited relatively higher mean cell volumes (V) and surface areas (S).

In the radial zone, the LTM also dominated findings for chondron morphological parameters; however, no significant differences among anatomical locations were detected (Table II). (Multiple-cell chondrons were observed only in the radial zone; therefore, chondron morphological parameters were identical to cell morphological parameters in the superficial and transitional zones.) In contrast to the rest of the knee, the number of cells per chondron (N_c) and matrix volume per chondron (M_c) appeared to be elevated in the LTM while chondron number density (N_{vc}) was less (Table II).

When data were averaged over the full tissue depth (Table III), significant differences tended to emerge where they had previously been seen in the superficial and transitional zones (Table I). Tissue-average cell surface area density (S_v ; Table III) was significantly greater in the MFC vs the mediocentral tibial plateau (MTM, MTN, and LTN), similar to findings in the superficial zone (Table I). On

Table II
Summary of results for chondron and matrix morphological parameters measured within the radial (deep) zone of cartilage from seven different locations in the adult human knee (mean \pm S.E.M.)

	N_c	N_{Vc} (10^3 mm^{-3})	M_c ($10^3 \mu\text{m}^3$)	n
MFC	6.3 \pm 1.9	1.7 \pm 0.4	780 \pm 200	8
LFC	5.4 \pm 1.5	1.7 \pm 0.4	730 \pm 230	6
PG	4.6 \pm 1.2	2.1 \pm 0.2	590 \pm 140	10
MTM	3.9 \pm 0.6	2.1 \pm 0.2	530 \pm 70	10
MTN	3.6 \pm 0.8	2.3 \pm 0.4	520 \pm 100	8
LTN	4.1 \pm 1.1	2.1 \pm 0.3	620 \pm 140	10
LTM	8.5 \pm 2.8	1.4 \pm 0.2	870 \pm 190	9

See Table I for definitions of locations (MFC, LFC, PG, MTM, MTN, LTN, and LTM). N_c = number of chondrocytes per chondron; N_{Vc} = number of chondrons per unit cartilage volume; M_c = matrix volume per chondron. No significant differences between locations were detected in these data.

On a tissue-average basis, the LTM exhibited significantly greater cell volume density (V_V), cell surface area density (S_V), and cell number density (N_V), and significantly smaller matrix volume per cell (M) than the rest of the tibial plateau (Table III), similar to findings for the transitional zone (Table I). The LTM also had greater tissue-average V_V and S_V compared to PG, and greater tissue-average S_V and N_V compared to LFC (Table III). The total number of cells and chondrons per unit articular surface (N_{AS} and N_{ASc} , respectively) showed significant variation among locations in the knee (Table III). Both N_{AS} and N_{ASc} tended to be largest at the LTN where cartilage was thickest, and smallest at the MTM where cartilage tended to be thinnest (Fig. 3).

Discussion

Although the present results may provide a reference point for evaluation of tissue repair treatments, current

methods of tissue engineering cannot yet reproduce the exact cell and matrix microstructure of healthy native tissue. Nor is it clear that they should, since repair tissue must develop and function under different metabolic and bio-mechanical constraints than native tissue. Nevertheless, it may be useful to identify tissue-averaged morphological parameters common throughout a range of anatomical locations, which could serve as benchmarks of "typical human articular cartilage morphology". Averages of present data taken over the full tissue depth (Table III) indicate several morphological parameters which do not vary among anatomical locations in the knee. Tissue-averaged chondrocyte volumes (V) and surface areas (S) exhibited no significant differences among anatomical locations: present results suggest that a "typical" adult human knee chondrocyte is described approximately by $V = 1650 \mu\text{m}^3$ and $S = 730 \mu\text{m}^2$. Assuming a spherical morphology, this corresponds to a cell diameter of about $15 \mu\text{m}$, which is roughly consistent with findings by different methods²⁰. The tissue-averaged number of cells per chondron (N_c) also showed no significant variation within the knee, at a typical value of 2.0 (Table III). Perhaps most interesting for tissue engineering purposes, tissue-averaged number of chondrons per unit volume (N_{Vc}) and matrix volume per chondron (M_c) also showed no variation throughout the knee around characteristic values of 4.6×10^6 chondrons per cm^3 and $224,000 \mu\text{m}^3$, respectively. Notably, "Stockwell's rule"²⁴, which suggests that the number of chondrocytes or chondrons beneath a unit area of articular surface (N_{AS} or N_{ASc}) are relatively constant, was not supported by present data; both parameters showed significant variation among anatomical locations in the knee (Table III).

Despite the statistically significant differences in cell and matrix morphology identified, it was also evident that certain anatomical locations within the knee never differed from one another, for any morphological parameters or tissue zones (Tables I–III). This suggests that different anatomical locations might be grouped together on the basis of similar

Table III
Summary of results for tissue-average cell, chondron, and matrix morphological parameters measured within cartilage from seven different locations in the adult human knee (mean \pm S.E.M.)

	V_V (%)	S_V (mm^{-1})	N_V (10^3 mm^{-3})	V (μm^3)	S (μm^2)	M ($10^3 \mu\text{m}^3$)	N_{AS} (10^3 mm^{-2})	n
MFC	1.7 \pm 0.2	7.8 \pm 0.1 $\dagger\dagger$	9.6 \pm 0.5	1750 \pm 190	820 \pm 70	104 \pm 5	23.7 \pm 1.8*	8
LFC	1.7 \pm 0.2	6.7 \pm 0.5*	8.7 \pm 0.4*	2000 \pm 260	780 \pm 70	115 \pm 6	23.8 \pm 2.0*	6
PG	1.5 \pm 0.1*	6.5 \pm 0.3*	9.7 \pm 0.5	1560 \pm 130	680 \pm 30	103 \pm 5	27.6 \pm 2.0 \dagger	10
MTM	1.2 \pm 0.1*	5.7 \pm 0.4*, \dagger	8.5 \pm 0.6*	1450 \pm 100	670 \pm 30	122 \pm 9*	18.6 \pm 1.8*, $\dagger\dagger$	10
MTN	1.2 \pm 0.1*	5.6 \pm 0.3*, \dagger	7.9 \pm 0.4*	1480 \pm 80	710 \pm 20	126 \pm 6*	24.2 \pm 1.8*	8
LTN	1.3 \pm 0.1*	5.5 \pm 0.4*, \dagger	8.1 \pm 0.4*	1600 \pm 70	690 \pm 40	126 \pm 9*	32.1 \pm 1.5**, \dagger	10
LTM	2.1 \pm 0.2**	8.9 \pm 0.6**	11.4 \pm 0.6**	1910 \pm 180	790 \pm 40	90 \pm 7**	26.6 \pm 1.8 \dagger	8
	N_c	N_{Vc} (10^3 mm^{-3})	M_c ($10^3 \mu\text{m}^3$)	N_{ASc} (10^3 mm^{-2})	n			
MFC	2.1 \pm 0.2	4.8 \pm 0.5	218 \pm 21	11.6 \pm 1.0*	8			
LFC	2.0 \pm 0.1	4.4 \pm 0.3	233 \pm 22	12.0 \pm 1.3	6			
PG	2.0 \pm 0.1	4.9 \pm 0.2	205 \pm 9	13.8 \pm 1.0	10			
MTM	1.9 \pm 0.1	4.7 \pm 0.5	231 \pm 22	10.4 \pm 1.4*	10			
MTN	2.0 \pm 0.1	4.1 \pm 0.3	251 \pm 18	12.8 \pm 1.6	8			
LTN	1.9 \pm 0.1	4.4 \pm 0.3	236 \pm 16	17.4 \pm 1.5**	10			
LTM	2.2 \pm 0.1	5.1 \pm 0.3	199 \pm 17	12.0 \pm 0.8*	8			

See Tables I and II for definitions of locations (MFC, LFC, PG, MTM, MTN, LTN, LTM) and morphological parameters (V_V , S_V , N_V , V , S , M , N_c , N_{Vc} , M_c). N_{AS} = total number of chondrocytes per unit articular surface; N_{ASc} = total number of chondrons per unit articular surface. Statistical comparisons were calculated between locations (not between tissue zones). Within the data set for each morphological parameter, data marked by asterisks (*) and daggers (\dagger) are significantly different ($P < 0.05$) from the data marked by double asterisks (**) and double daggers ($\dagger\dagger$), respectively.

cell and matrix morphologies. To investigate this, for each parameter and tissue zone, ANOVA was performed among the groups MFC + LFC (the femoral condyles), and MTN + LTN (the mediocentral tibial plateau); in both cases no significant variance was indicated. Although it appears from Tukey tests (Tables I–III) that the PG never differs from locations in the mediocentral tibial plateau, and that the LTN and LFC never differ from each other, at the level of ANOVAs these comparisons show significant variances in the transitional zone and when tissue-averaged parameters are compared. Present results may therefore be summarized in terms of only four distinct types of cartilage morphology in the knee, corresponding to the femoral condyles, the PG, the mediocentral tibial plateau, and the LTM. These groupings may in part represent cartilage adaptations to specific biomechanical roles. The femoral condyles serve similar mechanical roles as rotating convex surfaces with moving points of contact¹³. The tibial plateau functions as a concave surface with relatively constant contact points¹³; morphologic uniformity throughout the mediocentral tibial plateau may reflect cartilage adaptation to these roles. The PG and LTM, which could not be grouped together with any other anatomical locations in the knee, may have unique aspects of their biomechanics and local anatomy which result in relatively unique morphologies.

Cartilage thickness (Fig. 3) varied between anatomical locations in a manner seemingly independent of cell and matrix morphologies. Consistent with previous studies^{8,11}, significant thickness variations were observed among locations on the mediocentral tibial plateau. However, underlying cell and matrix morphologies were highly uniform. Articular cartilage thickness appears to be governed by a range of factors including the anatomical need for congruence between apposed joint surfaces¹², interactions with other tissues such as the meniscus⁸, and load-bearing^{8,16}. However, cartilage thickness is not trivially related to load-bearing: the tissue remodelling response to increased loading includes changes in joint surface areas¹¹ and site-specific differences in tissue mechanical properties^{7,8}. The relatively uniform cell and matrix morphology of cartilage amid changing tissue-scale geometry and function suggests fundamental constraints to cell-scale tissue organization. For example, cell metabolism must increase with matrix volume per cell at constant rate of turnover but cannot do so indefinitely due to transport limitations of nutrients, wastes, cytokines, and synthesized matrix molecules¹⁷. Chondrocytes also face a trade-off between decreased solute transport and increased mechanical stiffness associated with increased matrix density. These cell-scale constraints related to solute transport may underlie limitations to increased tissue thickness as a remodelling response to increased load^{8,11} and observations of decreasing mechanical stiffness with increasing cartilage thickness^{7,8,25}.

As previously described³, adult human knee cartilage has a substantially lower cell density than that which is typically observed in animals used for experimentation, and that typically used in tissue engineering procedures. These fundamental morphological differences must be kept in mind for the interpretation of relationships between experimental results and clinical problems. Since experimental animals are typically much younger than the 20 to 40-year-old human beings of the present study, these differences may be related to age in addition to species. Increasing acellularity of human cartilage with age² may be related to its diminishing capacity for repair, since fewer cells become

responsible for increasingly large areas of matrix. The low cell contents observed may represent limitations in terms of the number of cells which can be metabolically sustained in healthy articular cartilage in the human knee under normal conditions, and may be an unavoidable long-term constraint for tissue engineering procedures. Present findings may therefore provide a useful database for the improved understanding of cartilage metabolism and the tissue remodelling response to specific biomechanical environments, and aid in the improvement of strategies for cartilage tissue engineering.

Acknowledgements

This work was supported by grants from the 3R Research Foundation, Switzerland and the AO Foundation, Switzerland and by a Fellowship from the Arthritis Society of Canada (TMQ). We thank Prof U. Zollinger of the Department of Forensic Medicine at the University of Bern, Dr Eva Shimaoka, Nicole Kaufmann and Prasanna Perumbuli for assistance, and Dr A. Terrier for Fig. 2.

References

1. Poole AR, Pidoux I, Reiner A, Rosenberg L. An immunoelectron microscope study of the organization of proteoglycan monomer, link protein, and collagen in the matrix of articular cartilage. *J Cell Biol* 1982;93: 921–37.
2. Huch K. Knee and ankle: human joints with different susceptibility to osteoarthritis reveal different cartilage cellularity and matrix synthesis *in vitro*. *Arch Orthop Trauma Surg* 2001;121(6):301–6.
3. Hunziker EB, Quinn TM, Hauselmann HJ. Quantitative structural organization of normal adult human articular cartilage. *Osteoarthritis Cartilage* 2002;10(7):564–72.
4. Chen SS, Falcovitz YH, Schneiderman R, Maroudas A, Sah RL. Depth-dependent compressive properties of normal aged human femoral head articular cartilage: relationship to fixed charge density. *Osteoarthritis Cartilage* 2001;9(6):561–9.
5. Wong M, Wuethrich P, Egli P, Hunziker EB. Zone-specific cell biosynthetic activity in mature bovine articular cartilage: a new method using confocal microscopic stereology and quantitative autoradiography. *J Orthop Res* 1996;14(3):424–32.
6. Quinn TM, Grodzinsky AJ, Buschmann MD, Kim YJ, Hunziker EB. Mechanical compression alters proteoglycan deposition and matrix deformation around individual cells in cartilage explants. *J Cell Sci* 1998; 111:573–83.
7. Froimson MI, Ratcliffe A, Gardner TR, Mow VC. Differences in patellofemoral joint cartilage material properties and their significance to the etiology of cartilage surface fibrillation. *Osteoarthritis Cartilage* 1997;5(6):377–86.
8. Shepherd DE, Seedhom BB. Thickness of human articular cartilage in joints of the lower limb. *Ann Rheum Dis* 1999;58(1):27–34.
9. Cohen ZA, McCarthy DM, Kwak SD, Legrand P, Fogarasi F, Ciaccio EJ, *et al*. Knee cartilage topography, thickness, and contact areas from MRI: in-vitro calibration and in-vivo measurements. *Osteoarthritis Cartilage* 1999;7(1):95–109.

10. Franz T, Hasler EM, Hagg R, Weiler C, Jakob RP, Mainil-Varlet P. In situ compressive stiffness, biochemical composition, and structural integrity of articular cartilage of the human knee joint. *Osteoarthritis Cartilage* 2001;9(6):582–92.
11. Eckstein F, Faber S, Muhlbauer R, Hohe J, Englmeier KH, Reiser M, *et al.* Functional adaptation of human joints to mechanical stimuli. *Osteoarthritis Cartilage* 2002;10(1):44–50.
12. Simon WH, Friedenbergs S, Richardson S. Joint congruence. A correlation of joint congruence and thickness of articular cartilage in dogs. *J Bone Joint Surg Am* 1973;55(8):1614–20.
13. Iwaki H, Pinskerova V, Freeman MA. Tibiofemoral movement. 1: the shapes and relative movements of the femur and tibia in the unloaded cadaver knee. *J Bone Joint Surg Br* 2000;82(8):1189–95.
14. Eckstein F, Tieschky M, Faber S, Englmeier KH, Reiser M. Functional analysis of articular cartilage deformation, recovery, and fluid flow following dynamic exercise *in vivo*. *Anat Embryol (Berl)* 1999;200(4):419–24.
15. Waterton JC, Solloway S, Foster JE, Keen MC, Gandy S, Middleton BJ, *et al.* Diurnal variation in the femoral articular cartilage of the knee in young adult humans. *Magn Reson Med* 2000;43(1):126–32.
16. Vanwanseele B, Eckstein F, Knecht H, Stussi E, Spaepen A. Knee cartilage of spinal cord-injured patients displays progressive thinning in the absence of normal joint loading and movement. *Arthritis Rheum* 2002;46(8):2073–8.
17. Maroudas A. Biophysical chemistry of cartilaginous tissues with special reference to solute and fluid transport. *Biorheology* 1975;12:233–48.
18. Buckwalter JA, Mankin HJ. Articular cartilage: degeneration and osteoarthritis, repair, regeneration, and transplantation. *Instr Course Lect* 1998;47:487–504.
19. Vanwanseele B, Lucchinetti E, Stussi E. The effects of immobilization on the characteristics of articular cartilage: current concepts and future directions. *Osteoarthritis Cartilage* 2002;10(5):408–19.
20. Bush PG, Hall AC. The volume and morphology of chondrocytes within non-degenerate and degenerate human articular cartilage. *Osteoarthritis Cartilage* 2003;11(4):242–51.
21. Gundersen HJ, Bendtsen TF, Korbo L, Marcussen N, Moller A, Nielsen K, *et al.* Some new, simple and efficient stereological methods and their use in pathological research and diagnosis. *APMIS* 1988;96(5):379–94.
22. Cruz-Orive LM, Weibel ER. Recent stereological methods for cell biology: a brief survey. *Am J Physiol* 1990;258(4 Pt 1):L148–56.
23. Baddeley AJ, Gundersen HJG, Cruz-Orive LM. Estimation of surface area from vertical sections. *J Microsc* 1986;142:259–76.
24. Stockwell RA. Cell density, cell size and cartilage thickness in adult mammalian articular cartilage. *J Anat* 1971;108(3):583–5.
25. Lyyra T, Kiviranta I, Vaatainen U, Helminen HJ, Jurvelin JS. *In vivo* characterization of indentation stiffness of articular cartilage in the normal human knee. *J Biomed Mater Res* 1999;48(4):482–7.

Glossary

- MFC: medial femoral condyle.
 LFC: lateral femoral condyle.
 PG: patellar groove.
 MTM: medial tibial plateau (meniscus-covered).
 MTN: medial tibial plateau (not meniscus-covered).
 LTN: lateral tibial plateau (not meniscus-covered).
 LTM: lateral tibial plateau (meniscus-covered).
 V_v : chondrocyte volume per unit cartilage volume.
 S_v : chondrocyte surface area per unit cartilage volume.
 N_v : number of chondrocytes per unit cartilage volume.
 N_{vc} : number of chondrons per unit cartilage volume.
 V : chondrocyte volume.
 S : chondrocyte surface area.
 M : matrix volume per chondrocyte.
 N_c : number of chondrocytes per chondron.
 M_c : matrix volume per chondron.
 N_{AS} : total number of chondrocytes per unit articular surface.
 N_{ASC} : total number of chondrons per unit articular surface.